A modular microfluidic architecture for integrated biochemical analysis

Kashan A. Shaikh*, Kee Suk Ryu*, Edgar D. Goluch*, Jwa-Min Nam†, Juewen Liu‡, C. Shad Thaxton†, Thomas N. Chiesl§, Annelise E. Barron†§, Yi Lu‡, Chad A. Mirkin†, and Chang Liu*¶

*Department of Electrical and Computer Engineering, Micro and Nanotechnology Laboratory, and ‡Department of Chemistry, University of Illinois at Urbana–Champaign, Urbana, IL 61801; and †Department of Chemistry and Institute for Nanotechnology, and §Department of Chemical and Biological Engineering, Northwestern University, 2145 Sheridan Road, Evanston, IL 60201

Microfluidic laboratory-on-a-chip (LOC) systems based on a modular architecture are presented. The architecture is conceptualized on two levels: a single-chip level and a multiple-chip module (MCM) system level. At the individual chip level, a multilayer approach segregates components belonging to two fundamental categories: passive fluidic components (channels and reaction chambers) and active electromechanical control structures (sensors and actuators). This distinction is explicitly made to simplify the development process and minimize cost. Components belonging to these two categories are built separately on different physical layers and can communicate fluidically via cross-layer interconnects. The chip that hosts the electromechanical control structures is called the microfluidic breadboard (FBB). A single LOC module is constructed by attaching a chip comprised of a custom arrangement of fluid routing channels and reactors (passive chip) to the FBB. Many different LOC functions can be achieved by using different passive chips on an FBB with a standard resource configuration. Multiple modules can be interconnected to form a larger LOC system (MCM level). We demonstrated the utility of this architecture by developing systems for two separate biochemical applications: one for detection of protein markers of cancer and another for detection of metal ions. In the first case, free prostate-specific antigen was detected at 500 aM concentration by using a nanoparticle-based bio-bar-code protocol on a parallel MCM system. In the second case, we used a DNAzyme-based biosensor to identify the presence of Pb^{2+} (lead) at a sensitivity of 500 nM in <1 nl of solution.

laboratory-on-a-chip | microfluidic breadboard | polydimethylsiloxane

Advancement of microfabrication technology in the past few decades has enabled miniaturization and large-scale integration of complex systems, which has resulted in the availability of such products as analog/digital integrated circuits and powerful computers at affordable prices. The effects of miniaturization and integration reach far beyond the semiconductor industry. Microscale and nanoscale technologies are increasingly sought for purposes outside of traditional electronic applications.

One such example is the microfluidic laboratory-on-a-chip (LOC). Microfluidic technology promises to automate macroscale, bench-top laboratory protocols and encapsulate them in low-cost, portable systems. These systems benefit from reduced consumption of expensive reagents, precise manipulation of small volumes of fluid as low as a few picoliters, batch fabrication, and the ability to analyze a sample closer to the length scale of the subjects of interest (e.g., cells, protein, DNA). Important examples of LOC applications include sample preparation, cell manipulation, biomolecular separation (1, 2), PCR (1, 3), immunoassay-based detection (4, 5), and hybridization arrays (5, 6). Hence, LOCs have the potential to dramatically change the way biochemical analysis is performed for clinical diagnostics, environmental monitoring, pharmaceutical drug discovery, and chemical synthesis.

To successfully build an LOC, one must take into account a variety of different concerns, including biochemical compatibility, channel surface passivation/functionalization, optical transparency, ease of microfabrication, system integration, and cost of development. Significant time and expertise are required to resolve often nontrivial issues.

A gap currently exists between the developers and potential users of microfluidic chips. Potential users, especially those in the life sciences, generally do not have the means to manufacture or purchase custom microfluidic systems. Custom systems incur substantial costs because of both low volume production and the long development time associated with creating highly functional devices.

From the developers' perspective, two prevailing practices in LOC development contribute to the difficulties of building such a system. First, existing systems often use a monolithic approach, where chemical reactors, sensors, and actuators are integrated on a single chip. This approach requires a microfabrication process common to all components such that functionality may have to be compromised to build the device. Second, the components typically reside on a single plane, creating a need for elaborate channel routing to interconnect these components. Modifying one portion of monolithic and planar systems frequently entails rebuilding the entire system.

Our approach to narrowing the gap lies in the introduction of a system-level microfluidic architecture that allows for rapid customization with low cost by using materials satisfactory to both users and developers. The system reaches these goals by circumventing the obstacles encountered in conventional approaches.

Customizable Microfluidic System

We propose a fully customizable LOC architecture that is conceptualized on two levels: a single-chip level and a multiple-chip module system level.

At the single-chip level, components are separated into two fundamental categories: passive fluidic components and active electromechanical control structures. Passive components include chemical reactors and channels. Active components are sensors (e.g., flow rate, temperature, pressure) and actuators (e.g., pumps, valves, mixers). Active and passive structures are built separately on different physical layers.

Our methodology involves using a multifunctional chip (Fig. 1A) containing valves, pumps, mixers, and other active elements. The multifunctional chip is referred to as a microfluidic breadboard (FBB). It constitutes the foundation on which a second chip with passive components (e.g., routing channels and reaction chambers) is mated to complete the LOC (Fig. 1B). Fluid communication between these two layers is achieved via through-wafer ports in the FBB. We present a first-generation

---

ENGINEERING
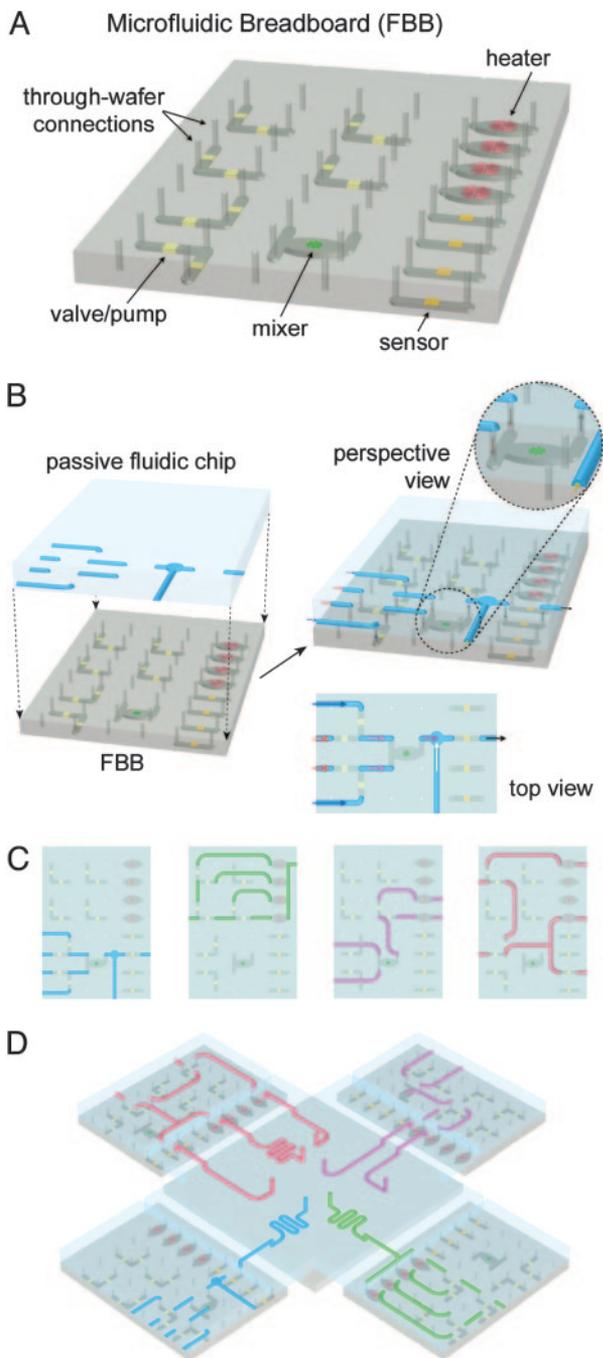
Fig. 1. Microfluidic breadboard system-level architecture. (*A*) Schematic diagram of a representative FBB consisting of electromechanical components and through-wafer fluidic connections. (*B*) A complete LOC can be built by bonding a passive fluidic chip with an FBB. (*Inset*) A perspective view emphasizing the fluidic communication between components on two levels. (*C*) Different functions may be realized by deploying different passive chips on the same FBB. (*D*) Multiple chips can be interconnected to form a larger system at the multiple-chip module level.

FBB implementing pneumatic valves and passive mixers in this article.

Although this distinction and separation may seem obvious, the implication is very significant. These two layers may use different sets of materials and can be manufactured at different locations by using different processes. Whereas the FBB chip would be built by foundries using sophisticated microfabrication processes, the passive chips could be made at the sites of use with fast turnaround time. The custom passive chips could also be produced in larger quantities by a dedicated foundry, thereby obviating the need for the user to fabricate a larger number of chips for one-time-use applications.

The FBB architecture can lead to an implementation methodology that reduces the cost and increases the speed of developing custom LOCs. For example, different LOC operations can be created by using a single FBB with a standard resource configuration. Realizing a new functionality only requires creating a new passive chip (Fig. 1*C*). Channel routing is vastly simplified in comparison to conventional planar microfluidic technology. A variety of FBBs accommodating complex functional elements in different standardized configurations could be made available at low cost when produced in large quantities.

The FBB methodology allows users of LOCs to make custom chips without relying on the expertise of fabricators. These custom chips can be designed and built rapidly, accelerating the pace of research and development.

Microfluidic chips with modular and nonplanar (3D) designs have been investigated in the past (7–10). Previously demonstrated methods require complex designs because of nonstandard segregation of passive and active components (7–9), have limited reconfigurabilty (8), and call for intricate fabrication and assembly of many small parts (7–10). Our design provides a viable solution for realizing custom, highly functional, and low-cost LOC systems.

In summary, the main advantages of the FBB architecture can be divided into two groups. From the user's perspective, the FBB allows for flexibility in choosing materials, rapid turnaround time, and low cost. Developers, on the other hand, benefit from scale of economy by providing standard parts for nonstandard applications.

Potential shortcomings of the FBB are an increase in dead volume and total channel path length. For example, the first-generation FBB has dead volume on the order of 25 pl, which is a fairly small price to pay to achieve rapid prototyping of systems with complex functionality. The dead volume and path length can be minimized by proper routing and channel design.

At the multiple-chip module level, individual FBBs (modules) performing specific functions can be interconnected in a reconfigurable manner to achieve a greater system-level operation (Fig. 1*D*). Fluid is transferred between modules via channels in micromachined connecting pieces. LOC systems with such detachable, interchangeable, and reconfigurable modules offer flexibility of design and operation. For example, individual modules can be removed from the system for purposes such as storage, transportation, and insertion into other systems.

With this architecture, we demonstrated systems for two separate biochemical applications by designing custom passive chips for use with a standard FBB. Each system was designed and built in 1 day because only the passive chips needed to be fabricated. The intent of these demonstrations is to show the utility of the architecture rather than complete LOCs.

Materials and Methods

Custom Passive Chip Fabrication. Passive polydimethylsiloxane (PDMS) chips were made by using the soft lithography method (11). PDMS prepolymer (10:1 ratio of base-to-curing agent, Dow-Corning Sylgard 184) was poured over a photoresist master, cured in a convection oven (90°C for 1 h), and then peeled off the master. Holes were punched with a sharpened 18-gauge luer stub to create inlet and outlet ports.

Photoresist masters were fabricated by spin-coating AZ 4620-positive photoresist (at 1,800 rpm for 30 s, EC101 Spinner, Headway Research, Garland, TX) on a Pyrex wafer to a thickness of 12 μm. The photoresist-covered wafer was then soft-
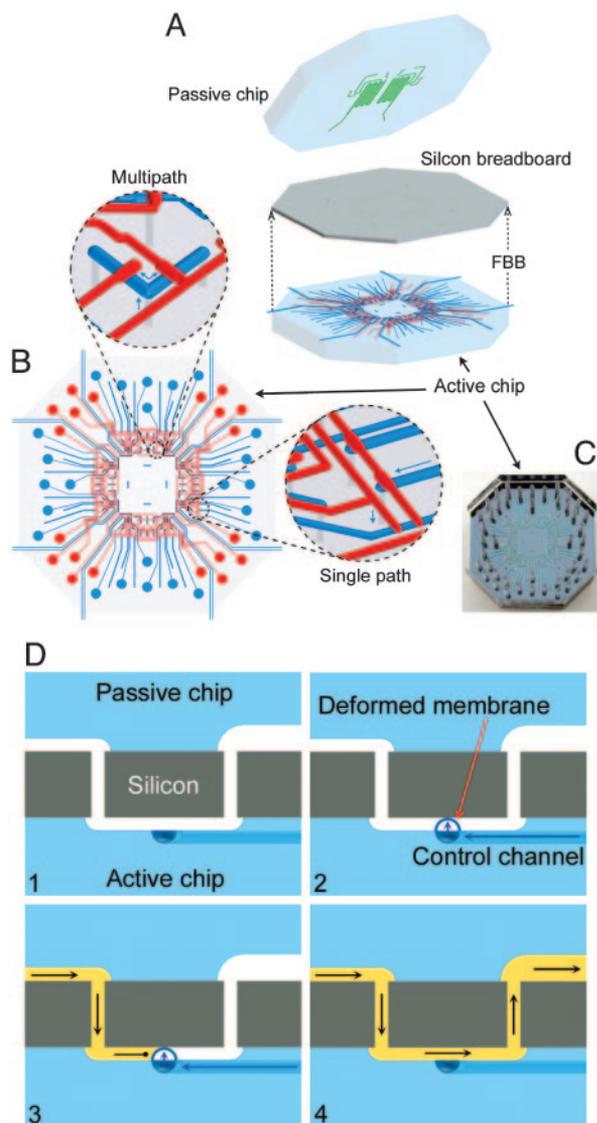
Fig. 2. First-generation FBB implementation. (*A*) The system was assembled by reversibly bonding a passive PDMS chip to the FBB, which consisted of an active PDMS chip bonded to an oxidized silicon wafer with through-wafer holes. (*B*) Pneumatically actuated valves were formed at the crossing of the pneumatic control (red) and fluid (blue) channels on the active chip. Single valves may be used to control sample loading, whereas multiple valves can be used for multipath switching. (*C*) An optical micrograph of a single LOC. Holes were punched in the PDMS chip to provide pneumatic connection ports to the valve control channels. (*D1*) Cross-sectional view of the LOC emphasizing the operation of a single valve. (*D2*) An empty channel is cut off by a thin PDMS membrane actuated via pneumatic pressure. (*D3*) Fluid may be filled up to the closed valve as air escapes through the PDMS. (*D4*) Releasing the pressure in the pneumatic control line opens the valve and allows the fluid to continue flowing.

baked (at 110°C for 2.5 min) to drive off the solvent, followed by UV exposure through a transparency mask and subsequent development. The wafer was hard-baked (110°C for 25 min) to form curved edges as a result of photoresist reflow. Masters were vapor-treated with chlorotrimethylsilane (Acros Organics, Geel, Belgium) inside a Petri dish to prevent adhesion of PDMS to the master after curing.

PDMS was selected for this first-generation implementation because of its excellent biocompatibility and low cost. However, other materials (polymers or glass) may be used in place of PDMS for selected applications.
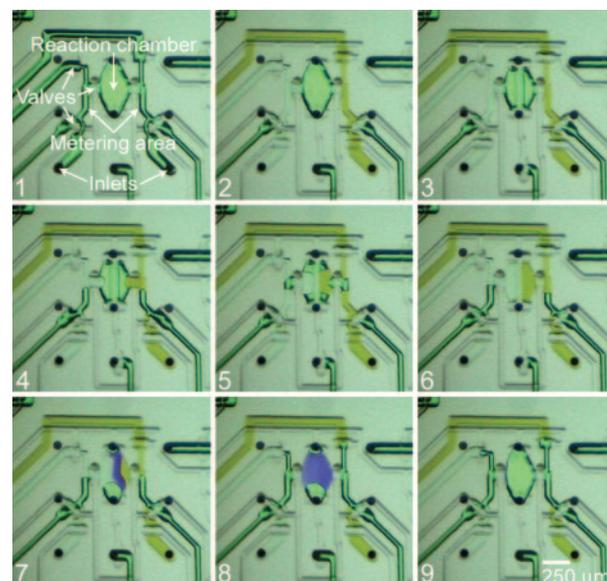
Fig. 3. Subsystem for mixing picoliter-scale volumes of fluid. Video frames illustrate the process by which precise volumes of fluid are loaded into either side of a microreactor and then mixed by diffusion. A concentrated solution of Cresol red (a pH indicator) in 0.1 M sodium hydroxide (NaOH) titrated with hydrochloric acid is loaded into the right half of the reactor (400 pl), stopped by a valve oriented along the length of the chamber. An equal volume of 0.1 M NaOH is loaded into the left half at the same time. The reactor is then isolated and the valve separating the fluids is opened to allow mixing, indicated by a color change from yellow to purple. Finally, the mixture is purged from the chamber and transferred to the passive chip on the opposite side of the FBB (not visible).

FBB Fabrication. The first-generation FBB (Fig. 2*A*) consists of an oxidized silicon chip with low dead-volume, through-wafer holes reversibly bonded to a PDMS piece with valves formed by multilayer soft lithography (12). The oxidized silicon breadboard was created by drilling holes through the wafer (50 μm diameter) via deep reactive ion etching using the Bosch process (Advanced Silicon Etcher, Surface Technology Systems, Newport, U.K.). Many different active elements, including heaters, mixers, and temperature sensors, can be incorporated on the silicon wafer by using microelectromechanical systems technology (13, 14).

Effective valves are critically important for reliable fluid control. PDMS chips with active components were fabricated by using multilayer soft lithography (Fig. 2*D*). This process involved bonding one layer with pneumatic control channels to another layer with fluidic channels. Thin membranes were formed at the crossing between channels on different layers, which could be pneumatically deformed to create valves that blocked the path of fluid in the fluidic channels. Fabrication consisted of partially curing PDMS prepolymer (5:1 ratio, 65°C for 15 min) on one master, defining the pneumatic control channels ($\approx$4 mm thick), peeling it off the master, and then punching access holes. The layer with fluidic channels was made by spin-coating (2,200 rpm, 60 s, EC101 Spinner, Headway Research) PDMS prepolymer (20:1 ratio) to a thickness of 60 μm over the photoresist mold and partially curing it (65°C for 15 min) to a soft state. The layer with control channels was aligned to the spin-coated PDMS and then bonded (90°C for 2 h). After initial bonding, the device was peeled from the fluidic channel master and further baked (90°C for 2 h) to complete the bonding.

Control Hardware. Pressurized nitrogen was used to load and transport fluids (7–20 kPa), and operate valves (83–103 kPa) in the system. An array of off-chip solenoid valves (Cole-Parmer,

ENGINEERING
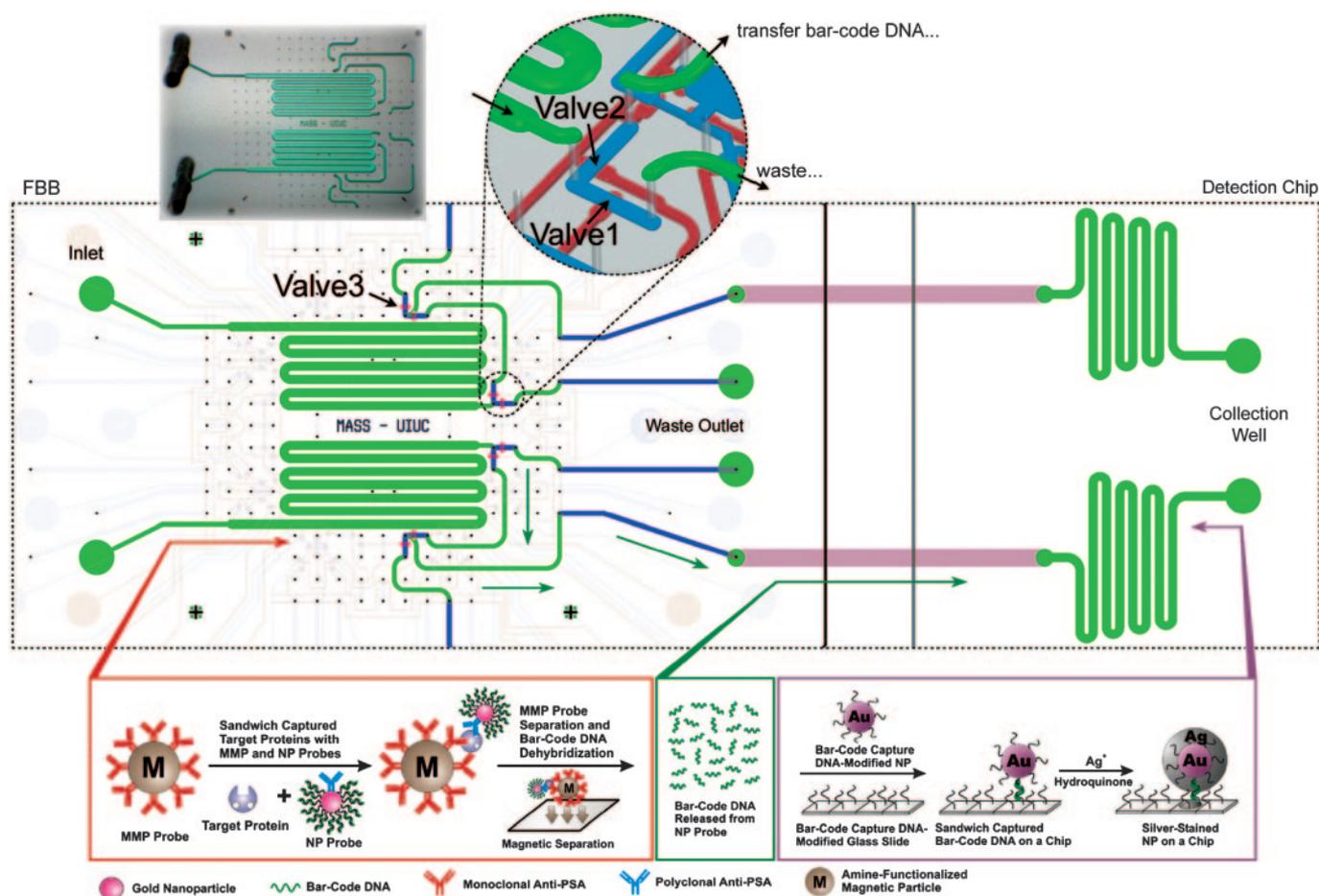
Fig. 4. System design for the detection of fPSA with the BBC protocol. The PSA is sandwich-captured and separated in the first stage of the device (because of an applied magnetic field) by flowing solutions from the inlet to the waste outlet with valve 2 closed and valve 1 open. Indirect amplification is provided by bar-code DNA that is released from the sandwich and transferred from the FBB to the detection chip. Valve 1 and valve 3 are closed, whereas valve 2 is opened to allow the bar-code transfer. The bar codes attach to the surface of the DNA-modified detection chip and are sandwiched with gold NPs that are then silver-stained to provide a direct optical readout of the result.

Vernon Hills, IL) controlled the pressure in each connected channel. The solenoid valves were interfaced with a data acquisition card (National Instruments, Austin, TX) and remotely controlled by using LABVIEW (National Instruments).

Basic Fluidic Operations

Many different fluid manipulations are necessary in LOC systems. Two essential operations are the control of fluid movement and control of fluid interactions. The following sections describe how these operations are accomplished within the framework of FBB.

Control of Fluid Movement. An array of pneumatic valves was created on the FBB (Fig. 2B) to provide flow control in single fluid paths as well as in multiple paths. Valves controlling single paths were useful for sample loading, reactor isolation, and maintenance of flow consistency across parallel channel networks. Multipath valve control was used to select between different channels. As an example, fluid flowing into a waste channel could be halted and then diverted into another channel for further processing and analysis. Because PDMS is a gas-permeable material, fluid was routinely filled up to a closed valve by displacing air through the PDMS. Indeed, one of the advantages of using PDMS is that trapped bubbles can be purged by closing a valve and applying pressure to the fluid surrounding the bubble. The valves were arranged symmetrically around each

side of the FBB such that channel routing was simplified for the passive chips.

Pneumatic valves were always dead-end filled with water and actuated with 83–103 kPa of pressure, depending on the back-pressure in the fluidic channels. The pressure necessary for closing a valve was higher than other published values (12) because of an increased PDMS membrane thickness (60 μm). This increase was necessary to ensure that the valve restoring force was large enough to reliably overcome FBB surface stiction and the surface tension of various fluids. Valves could be actuated and sealed within 1 ms and released in anywhere from 1 ms to 1 s depending on the properties of the fluid surrounding the valve. The reliance on a passive mechanism for opening a closed valve is one of the drawbacks of using valves formed by multilayer soft lithography.

Control of Fluid Interactions: Picoliter-Scale Microreactor. One of the most common needs for LOCs is a microreactor that mixes small volumes of two or more different solutions. Accordingly, a valve-assisted mixing subsystem was built on the FBB. Fig. 3 contains frames from a video that shows a pH-sensitive, colorimetric acid-base reaction used to demonstrate the operation of the mixing system (see Movie 1, which is published as supporting information on the PNAS web site). A basic solution was saturated with Cresol red (a pH indicator) and then titrated with an acidic solution. This indicator fluid (yellow colored) and a
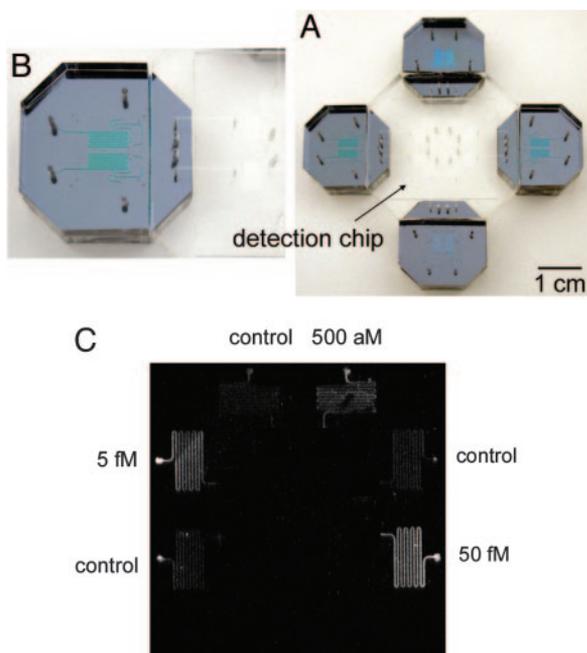
Fig. 5. Fabricated device and testing results for the detection of fPSA. (*A*) The system is capable of concurrently performing eight different BBC tests by connecting four identical chips to a centralized detection chip. (*B*) Each chip can run two simultaneous tests. (*C*) fPSA was detected at concentrations ranging from 50 fM to 500 aM based on the intensity of scattered light off the silver-stained NPs.

Fig. 6. Low-level Pb^{2+} (lead) detection with a DNAzyme-based fluorescent biosensor. (*A*) The DNAzyme biosensor is made of a cleavable substrate annealed with an enzyme strand. A fluorescent probe (FAM) located on the 5′ end of the substrate is quenched by probes (Dabcyl) on both strands until the presence of lead causes the enzyme strand to cleave the substrate, resulting in increased fluorescence. (*B*) The biosensor was mixed with samples containing lead by using the picoliter-scale reactor on the FBB. Four samples were processed simultaneously in four separate reactors. (*C*) The samples were then transferred to the detection area on the passive chip. (*D*) Lead was detected from 10 μM to 500 nM by measuring the fluorescence intensity of the four results.

basic solution were flowed into separate sides of the valve-controlled metering channels where specific volumes were measured. The measured volumes (defined by the channel geometry) were then introduced into either side of the microreactor, separated by a valve oriented along the length of the chamber. This process was repeated until the desired volumes had been loaded in the reactor (maximum of 400 pl in each half). Closing the chamber isolation valves and opening the central valve allowed the fluids to combine and mix by diffusion, producing a color change from yellow to purple. After desired mixing was achieved, the mixture was transported out of the chamber through FBB channels connecting to a passive chip.

Results and Discussion

Two different passive chips were designed to implement two different functions, both using the same FBB base design. These demonstrations are intended to illustrate the reconfigurability, functionality, and rapid prototyping capability of LOC systems based on this architecture.

Bio-Bar-Code (BBC) Amplification Assay for Prostate-Specific Antigen (PSA). The first chip was used to detect ultra-low levels of free (unbound) PSA (fPSA) by using the BBC assay (15). The presence of PSA in a person's bloodstream can be used as an indicator of both prostate and breast cancer (16, 17). For total PSA (tPSA) levels <4 μg/liter (< 118 pM), the ratio of fPSA-to-tPSA has been shown to be a more sensitive indicator than tPSA alone (18). An ultrasensitive and specific method like the BBC (4 orders of magnitude more sensitive than conventional techniques) can help provide reliable screening and diagnosis at the extremely low levels of fPSA (10–30% of tPSA). We achieved fPSA detection at 500-aM concentration with our chip, which was designed to allow two separate BBC tests to be run concurrently on one FBB (Fig. 4).

A particular test involved several steps. All probes were

prepared according to published methods (15). Samples were comprised of fPSA in 0.1 M PBS. The sample (4 μl) was premixed with an aqueous solution containing magnetic microparticles (MMPs; 8 μl, 3 mg/ml, 1 μm diameter) functionalized with monoclonal anti-PSA antibodies and incubated (37°C for 30 min) to specifically couple any fPSA molecules present in the liquid to the MMPs. This mixture (1 μl) was then introduced onto the chip via the inlet and was flowed through the separation channel to the waste outlet while an applied magnetic field immobilized the MMPs on the channel surface. All channels in the separation area were coated with polynhydroxyethylacrylamide (polyDuramide) to minimize nonspecific binding of particles to the channel walls. Valve 2 was closed to guide the solution to the waste and prevent it from entering the network leading to the detection area. Gold nanoparticles (NPs; 1 μl, 200 pM, 30 nm) functionalized with hybridized oligonucleotides (BBCs; 5′-ACACAACTGTGT-TCACTAGCGTTGAACGTGGATGAAGTTG-3′) and polyclonal anti-PSA antibodies were then bound to the immobilized PSA by flowing the NP solution through the separation channel to the waste outlet. Flow was stopped at regular intervals to increase binding efficiency. The separation channel was then washed by flowing 3 μl of 0.1 M PBS to remove any nonspecifically bound NPs. For each target PSA sandwiched between one MMP and at least one NP, hundreds of bar-code DNA molecules were released (19), which provided indirect amplification. With the magnetic field still applied, deionized water (1 μl, 18 MΩ) was flowed through the separation channel to dehybridize the bar-code DNA and thus release the DNA from the NPs. By closing valve 1 and valve 3

and opening valve 2, the bar-code molecules were transferred to the detection area where they were collected in a well.

Roughly 0.5 μl of 0.1 M PBS was introduced into the well and allowed to mix with the bar-code solution. This mixture was then flowed from the collection well through the detection area to hybridize the bar codes with complementary strands containing half the bar-code sequence (5′-SH-[CH$_2$]$_6$-A$_{10}$-CAACT-TCATCCACGTTCAAC-3′) already immobilized on a glass slide. Gold NPs functionalized with oligonucleotides comprising the other half of the bar-code sequence (1 μl, 500 pM, 13 nm, 5′-GCTAGTGAACACAGTTGTGT-A$_{10}$-[CH$_2$]$_3$-SH-3′) were then flowed through the detection area to label the bar codes in a sandwich assay format. A 3-μl wash with 0.3 M PBS followed by a 1-μl secondary wash (0.15 M NaNO$_3$ in deionized water) cleansed the detection area before flowing silvering solution for 5 min. Silver deposited on the NPs and subsequently wrapped around them, providing an amplified signal for optical detection. The result was a gray-colored area in the shape of the detection channel with an intensity related to the concentration of fPSA in the sample. A Verigene ID system (Nanosphere, Northbrook, IL) was used to quantify the light scattering off the silvered pattern.

Two samples were typically tested simultaneously with a single chip (Fig. 5B): one with a known concentration of fPSA, and the other a control without fPSA. Four of these chips were connected to a centralized detection slide, resulting in a multiple-chip module system capable of running eight concurrent tests (Fig. 5A). Concentrations ranging from 50 fM to 500 aM were detected on a single detection slide (Fig. 5C). Uniformity between tests was maximized because of the parallel nature of the system. Although results using a more complex sample are not presented here, we have promising data indicating that the polyDuramide is indeed effective at preventing nonspecific binding when testing for fPSA in a serum solution. The poly-Duramide was flowed through the channels in both the passive and active chips. It is possible to make the entire system biocompatible.

Low-Level Lead Detection. A second passive chip connected to the FBB formed a system used to detect the presence of Pb^{2+} (lead) with a DNAzyme-based biosensor (20, 21). Low-level lead exposure can contribute to a number of different adverse health effects. When in the bloodstream it is considered toxic above concentrations of 480 nM (22). The Pb^{2+}-specific DNAzyme biosensor consists of an enzyme strand and a cleavable substrate strand with a fluorescent probe attached to the 5′ end (Fig. 6A). Two fluorescent quenchers (Dabcyl) reside in close proximity to the probe (one on the 3′ end of the substrate and the other on the 5′ end of the enzyme strand), which yields low-level background fluorescence. In the presence of lead, the substrate is cleaved by the enzyme, which releases the cleaved fragments and results in increased fluorescence signal.

Lead detection was performed by using the picoliter-scaled mixing subsystem on the FBB (Fig. 6B). The biosensor (2 μM concentration) was introduced in one side of the system, whereas a solution (100 mM NaCl in 15 mM Tris acetate buffer, pH 8.2) containing lead was introduced in the other side. Both solutions completely filled their respective halves of the reaction chamber as per the method previously outlined. The chamber was then isolated from the inlets by actuating valves on either side of the chamber, resulting in a volume in each half of the chamber of 400 pl. Releasing the separation valve allowed the solutions to begin mixing at the interface between the two solutions. After 5 min sufficient diffusive mixing was achieved, and the uniform mixture was transferred to the detection channels in the passive chip (Fig. 6C). Fluorescence intensity was measured by exciting the mixture at a wavelength of 480 nm and detecting emission >510 nm by using a fluorescence stereomicroscope (MZ FLIII, Leica Microsystems, Wetzlar, Germany) in conjunction with a cooled charge-coupled device color camera (Leica DFC480). Four different solutions with varying lead concentrations were reacted with the biosensor in four parallel chambers simultaneously. Using this scheme we detected lead concentrations ranging from 10 μM to 500 nM (Fig. 6D). One fluorescence snapshot was taken for all four samples at the same time, eliminating variability in the measurement between samples.

Both the BBC detection and the lead sensor implementations presented here could be optimized in part by integrating more active components on the FBB.

1. Lagally, E. T., Medintz, I. & Mathies, R. A. (2001) *Anal. Chem.* **73,** 565–570.
2. Han, J. & Craighead, H. G. (2000) *Science* **288,** 1026–1029.
3. Kopp, M. U., de Mello, A. J. & Manz, A. (1998) *Science* **280,** 1046–1048.
4. Wang, J., Ibanez, A. & Chatrathi, M. P. (2003) *J. Am. Chem. Soc.* **125,** 8444–8445.
5. Selvaganapathy, P. R., Carlen, E. T. & Mastrangelo, C. H. (2003) *Proc. IEEE* **91,** 954–975.
6. Tillib, S. V. & Mirzabekov, A. D. (2001) *Curr. Opin. Biotechnol.* **12,** 53–58.
7. Verpoorte, E. M. J., Van Der Schoot, B. H., Jeanneret, S., Manz, A., Widmer, H. M. & De Rooij, N. F. (1994) *J. Micromech. Microeng.* **4,** 246–256.
8. Kikutani, Y., Horiuchi, T., Uchiyama, K., Hisamoto, H., Tokeshi, M. & Kitamori, T. (2002) *Lab Chip* **2,** 188–192.
9. Hofmann, O., Niedermann, P. & Manz, A. (2001) *Lab Chip* **1,** 108–114.
10. Schabmueller, C. G. J., Koch, M., Evans, A. G. R. & Brunnschweiler, A. (1999) *J. Micromech. Microeng.* **9,** 176–179.
11. Duffy, D. C., McDonald, J. C., Schueller, O. J. A. & Whitesides, G. M. (1998) *Anal. Chem.* **70,** 4974–4984.
12. Unger, M. A., Chou, H.-P., Thorsen, T., Scherer, A. & Quake, S. R. (2000) *Science* **288,** 113–116.
13. Ryu, K., Shaikh, K., Goluch, E., Fan, Z. & Liu, C. (2004) *Lab Chip* **4,** 608–613.
14. Chen, J. & Liu, C. (2003) *J. Microelectromech. Syst.* **12,** 979–988.
15. Nam, J.-M., Thaxton, C. S. & Mirkin, C. A. (2003) *Science* **301,** 1884–1886.
16. Ferguson, R., Yu, H., Kalyvas, M., Zammit, S. & Diamandis, E. (1996) *Clin. Chem.* **42,** 675–684.
17. Black, M. H., Giai, M., Ponzone, R., Sismondi, P., Yu, H. & Diamandis, E. P. (2000) *Clin. Cancer Res.* **6,** 467–473.
18. Stephan, C., Jung, K., Lein, M., Sinha, P., Schnorr, D. & Loening, S. A. (2000) *Cancer Epidemiol. Biomarkers Prev.* **9,** 1133–1147.
19. Nam, J.-M., Stoeva, S. I. & Mirkin, C. A. (2004) *J. Am. Chem. Soc.* **126,** 5932–5933.
20. Li, J. & Lu, Y. (2000) *J. Am. Chem. Soc.* **122,** 10466–10467.
21. Liu, J. & Lu, Y. (2003) *Anal. Chem.* **75,** 6666–6672.
22. Centers for Disease Control (1991) *Preventing Lead Poisoning in Young Children* (U.S. Department of Health and Human Services, Centers for Disease Control, Atlanta).